Macromolecular Research, Vol. 14, No. 6, pp 617-623 (2006)

Surface and Dielectric Properties of Oriental Lacquer Films Modified by UV-Curable Silicone Acrylate

Jin-Who Hong and Hyun-Kyoung Kim*

Department of Polymer Science & Engineering, Chosun University, Gwangju 501-759, Korea

Received July 20, 2006; Revised October 24, 2006

Abstract: In order to achieve an oriental lacquer (OL) film with a thick consistency, UV-curable silicone acrylate (SA) was added to OL by a dual curing process. The addition of 5 wt% UV-curable SA to the OL formulation enabled the preparation via a single drying step of a 77 μm-thick film exhibiting excellent surface properties. FTIR-ATR was used to investigate the effect of UV-curable SA on the behavior of film formation during curing, and the relaxation behavior of the produced films was investigated by dielectric spectroscopy. Dielectric properties were measured in the frequency range 10^{-2}-10^{5} Hz at various temperatures between -100 and 200 °C. The results demonstrated that OL modified by UV-curable SA has a higher glass transition temperature and stronger secondary relaxation at a lower temperature than the conventional OL system. The OL film modified with UV-curable SA was presumed to be harder at the surface and tougher than conventional OL film.

Keywords: oriental lacquer, silicone acrylate, dielectric properties, surface properties, UV-curable.

Introduction

Oriental lacquer is a biodegradable, natural product which has been used for protective and decorative coatings since the fifth century B.C. The resinous sap of the Rhus vernicifera tree is obtained during the collection of natural rubber. The sap is a water-in-oil type of emulsion, composed of urushiol (60-65%), gummy substances (incorporating mono-, oligo-, and polysaccharides) (4-7%), glycoproteins (2-3%), and laccase (*p*-quinol oxido-reductase; enzyme) (0.2-1%). After filtration and traditional purification, the lacquer can be used directly as a coating material.[1-6] It is the hardening process of the oriental lacquer that distinguishes it from synthetic coatings: rather than solvent evaporation, the primary curing mechanism for oriental lacquer is an oxidation-induced polymerization. Another unusual feature of oriental lacquer is that it cures to its hardened state most efficiently at moderate temperatures in the presence of air at relative humidity of greater than 70%.[7-10]

The durability and beauty of oriental lacquer has meant that during the long period since its discovery, many different types of item have been lacquered with it, from desks and other furniture pieces to sword scabbards, temple pillars and boxes, and countless other items both formal and personal. However, the widespread use of this oriental lacquer is limited by some disadvantages: the low yield of sap from lacquer trees; the labor-intensive method of sap collection; the low drying rate because it is controlled by diffusion of laccase or oxygen, preventing drying at a higher temperature; the allergic reactions in some who come in contact with the lacquer; and the repeated rubbing and drying (typically 5-10 times) required to produce a high gloss and highly cross-linked durable surface.[1]

In this study, UV-curable silicone acrylate (SA) was introduced to an oriental lacquer by a dual curing method to achieve a thick oriental lacquer film. The effect of the inclusion of UV-curable SA on the surface morphology and properties of the oriental lacquer were investigated. In addition, the distribution of UV-curable SA in the oriental lacquer film was observed at the film-air (FA) and film-substrate (FS) interfaces using FTIR-ATR spectroscopy. The effects of dual curing on the dielectric relaxation of oriental lacquer films were also investigated.

Experimental

Preparation of Lacquer Films. Chinese raw urushi was filtered using a traditional filter paper called *chilji*. To prepare the purified oriental lacquer (POL, *jungjeotchil*), the filtered raw oriental lacquer (*sangochil*) was stirred at 60 rpm in an open vessel (150 mm diameter × 150 mm height) for 2 h and then at 45 °C for 5 h. The purification procedure for *jungeotchil* is based on the traditional method in which the main objective is to reduce the water content of the raw

*Corresponding Author. E-mail: hkkim@chosun.ac.kr

urushi from 25-35% to 3-6%. The POL sample, coated on PET film at a thickness of 10 μm, was dried for 1 day at room temperature and 75 ± 5% RH. The POLSA sample containing the UV-curable SA (5%) and photoinitiator (0.5%), coated on PET film at a thickness of 77 μm, was cured with 380 W/cm^2 light from a medium-pressure mercury lamp (80 W/cm) for 20 s using conventional UV equipment, and then dried for 1 day at room temperature and 75 ± 5% RH. The chemical structure of the silicone acrylate (α,ω-acryloxy organofunctional polydimethylsiloxane; Goldschmidt) used in the experiment is shown in Figure 1. The photoinitiator, 2-hydroxy-2-methyl-1-phenyl-propane-1-one, was supplied by Ciba-Geigy.

Measurements. Pencil and pendulum hardnesses were measured using standard methods (ASTM D 3363 and D 4366, respectively). In addition, the gloss (ASTM D 523) of the oriental lacquer was measured on Leneta test papers using a gloss meter from Sheen. The values reported here represent the averages from ten measurements. The surface tension of the oriental lacquer films was estimated by Lewis acid-base theory using contact-angle data with water, formamide, and diiodomethane as wetting liquids. For each liquid, five microdrops were placed on the surface of the films, and contact-angle readings were taken from both the left and right sides of the liquid-air-solid interface.

The morphology of the oriental lacquer films was studied using scanning electron microscopy. FTIR-ATR spectra were recorded on a Bruker IFS-85 spectrometer, which was continuously purged with purified air that was free of carbon dioxide and water (using a desiccant air dryer from New Technics). To enhance the signal-to-noise ratio, each of the reference and sample spectra represent the average of 128 scans recorded at 8 cm^{-1} resolution. The spectrometer was equipped with a variable-angle ATR attachment, and a 45° parallelogram prism of ZeSe was used as an internal reflection element.

A TA Instruments dielectric analyzer DEA 2970 coupled with a 2100 thermal analyzer was used to obtain the dielectric properties of the samples. Parallel-plate sensors were used in the dielectric experiments. The DEA module provided real-time quantitative calculations of the properties for 15 frequencies in the range 10^{-2}-10^5 Hz at various temperatures from -100 to 200 °C using a heating rate of 0.5 °C/min. The module internally converted the measured sample response (capacitance C, conductance $1/R$, and phase-angle shift) into permittivity and loss factor using

$$\varepsilon' = \frac{Cd}{A\varepsilon_o} \qquad \varepsilon'' = \frac{d}{RA2\pi f\varepsilon_o}$$

where d is the sample thickness, ε_o is the permittivity of a vacuum (8.854×10^{-12} F m^{-1}), A is the metallized electrode area, f is the frequency of the excitation, and R is the resistance of the sample.

Results and Discussion

Surface Morphology and Physical Properties. The effects of the inclusion of UV-curable SA on the surface morphology and physical properties of the oriental lacquer films are summarized in Figure 2 and Table I. When 5 wt% of UV-curable SA was added into the oriental lacquer formulation, we were able to produce a 77 μm-thick film (POLSA) with excellent surface properties using a single drying step. Figure 2(b) shows the serious wrinkles that were observed on the FA interface of the POL sample when the film thickness is above 10 μm, which are due to the prevention of oxygen diffusion at core and the FS interface as the film thickness increases, resulting in a gradient in the curing profile: well cured at the FA interface and poorly cured at the FS interface. In contrast, no wrinkles were observed on the POLSA coating film even for a 77 μm film thickness. It is thought that the excellent gas permeability of the UV-curable SA expands the boundary area of oxygen transportation zone from the surface to the core. The conventional oriental-lacquer curing procedure requires rubbing and drying up to 10 times in order to achieve a 77 μm-thick film with a high gloss and highly cross-linked durable surface, so our dual curing system can be regarded as a significant improvement for the oriental lacquer industry, given that the drying time can be decreased sevenfold.

It is notable that the pencil hardness increased whereas the pendulum hardness decreased when the UV-curable SA was added into the oriental lacquer formulation, which indicates that the addition of UV-curable SA increases the degree of cure at the surface (as reflected by the bulk pencil hardness test) but decreases the degree of cure at the core (as reflected by the pendulum hardness test). From the increase in pencil hardness it is presumed that UV modification of oriental lacquer by dual curing leads to a high cross-link density at the surface. In contrast, the oriental lacquer can exhibit a high absorption in the UV spectrum from 250 to 450 nm, thereby decreasing the effect of the photoinitiator in the core region. It is also observed that the gloss of the POLSA film is

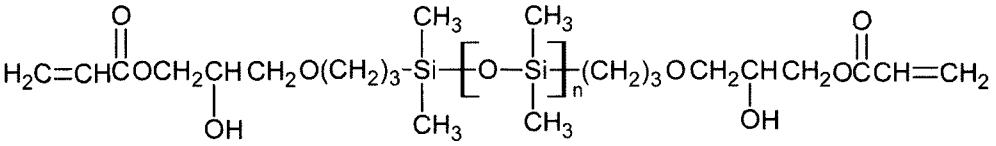

Figure 1. The chemical structure of UV-curable silicone acrylate.

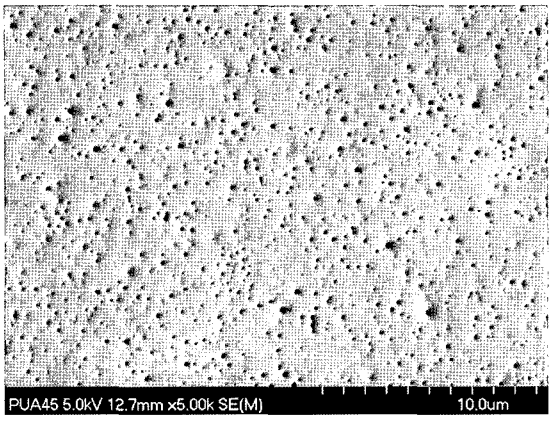

(a)

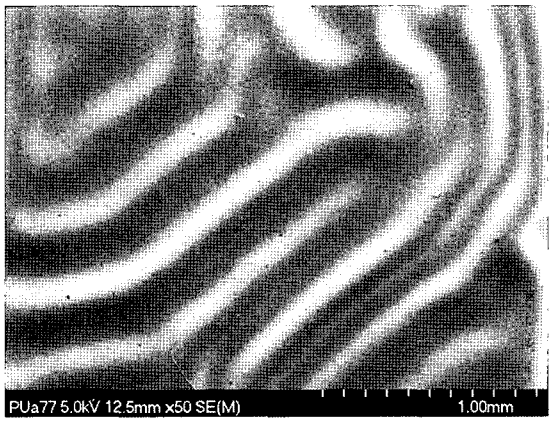

(b)

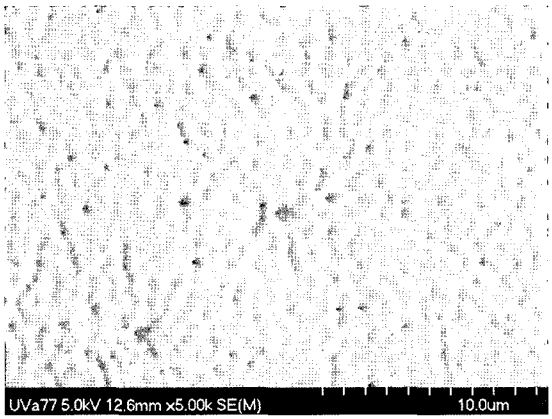

(c)

Figure 2. Scanning electron micrographs of the oriental lacquer films at the film-air interfaces: (a) 10 μm-thick POL film, (b) 77 μm-thick POL film, and (c) 77 μm-thick POLSA film.

Table I. Surface Properties of Two Oriental Lacquer Films

Sample	Film Thickness (μm)	Hardness		Gloss (%)	Surface Tension (mN/m)
		Pencil	Pendulum (s)		
POL	10	2B	128	100.8	47.07
POLSA	77	1B	83	112.3	37.95

higher than that of the POL film. In principle, coating gloss is a complex phenomena resulting from the interaction between light and the surface of the coating, and is affected strongly by surface roughness. Therefore, one would expect that the increased gloss of the POLSA film is due to its more-uniform surface morphology than the POL system. As shown in Figure 2, the surface of the POL film had pinholes of 0.1-0.2 μm diameter, which is due to polysaccharide particles composed of polymerized urushiol and glycoproteins. The number of pinholes at the surface of the POLSA film is less than that of the POL film, and we also observed that the surface morphology of the POLSA film is more uniform than that of the POL film, which increases the gloss of the former. Moreover, the surface energy of the POL film is higher than that of the POLSA film, which is presumably related to the existence of polysaccharides in the top layer of the former. According to Kummanotani,[5,6] the coating network of the the POL film is surrounded by hydrophilic polysaccharides which would increase the surface energy of the film. Therefore, one would expect that the UV irradiation on the POLSA film and presence of hydrophobic siloxane groups in the coating network would reduce the existence of the polysaccharides in the surface of coating film, resulting in an increase of the contact angle and a decrease of the surface energy.

We now consider how the addition of UV-curable SA into the oriental lacquer affects film formation, particularly the distribution of the UV-curable SA in the coating network of the POLSA film. Figure 3 shows the FTIR-ATR spectra of POL and POLSA films. The most pronounced changes in the ATR spectra induced by adding the UV-curable SA into the POL film occurred at 1258, 1022, and 810 cm^{-1}, which are characteristic of Si-CH_3 symmetric deformation, Si-O-Si asymmetric stretching, and a C-H deformation mode of the acryl groups, respectively. The detection of a UV-curable SA group in the FTIR-ATR spectra is not surprising, although

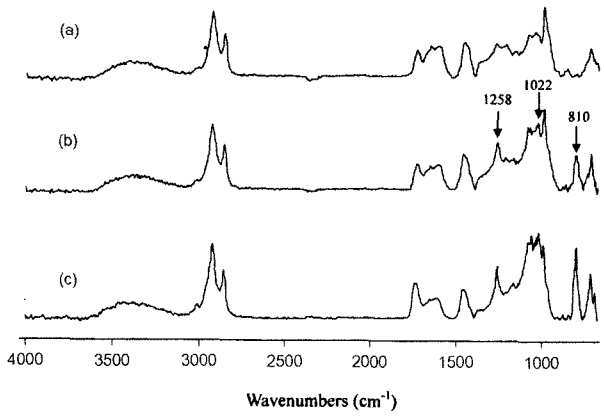

Figure 3. FTIR-ATR spectra of the oriental lacquer films: (a) POL at the film-air interface, (b) POLSA at the film-air interface, and (c) POLSA at the film-substrate interface.

it should be noted that the IR bands from UV-curable SA and unreacted acrylic double bonds are more enriched at the FS interface. This result suggests that the reduced pendulum hardness for the POLSA film compared to the POL film is due to the presence of unreacted UV-curable SA at the FS interface. It is also apparent that we could prepare the thick oriental lacquer film using a one-step coating procedure because the UV-curable SA is distributed all over the films (even to the FS interface), so that the diffusion of oxygen is possible to the FS interface. IR spectral vibrations of the POLSA film are similar to those of the POL film with the exception of the specific peaks related to the UV-curable SA, although there are differences in the absolute intensities of the peaks. This suggests that the POLSA film is cross-linked by an oriental-lacquer curing mechanism consisting of two parts: (1) the laccase-catalyzed dimerization of the catechol rings of the 3-*n*-alkylcatechols, and (2) the oxidative curing of the unsaturated aliphatic side chains. Although we could not elucidate the dual curing mechanism of the POLSA film in detail, it can be assumed that UV irradiation of the oriental lacquer for only 20 s would not affect adversely the curing of the lacquer.

Dielectric Relaxations. To explore the changes in microstructure resulting from the addition of UV-curable SA into oriental lacquer, we investigated the loss factor, ε'', of the oriental lacquer films as functions of temperature and frequency. Figures 4 and 5 show the clear contrast in the relaxation behavior between the two materials. Relaxation peaks at around -50, 1, and 50 °C in the frequency domain were observed for the POL film, and peaks at around -100, -50, and 75 °C were observed for the POLSA film. In order to assign the various relaxation peaks in Figures 4 and 5, Arrhenius plots of log-frequency versus inverse-temperature were derived from the frequency- and temperature-dependent dielectric-loss curves.

The activation energies of relaxations for two oriental lacquer films were determined from the slopes of the plots (Figure 6), and are summarized in Table II. The apparent activation energies of relaxation peaks for the POL film at around 50 and 1 °C were 60 and 19 kcal/mol, respectively, suggesting that the relaxation peak at 1 °C is due to secondary relaxation (β relaxation) while the peak at 50 °C is due to the glass transition (α relaxation). Unfortunately, the

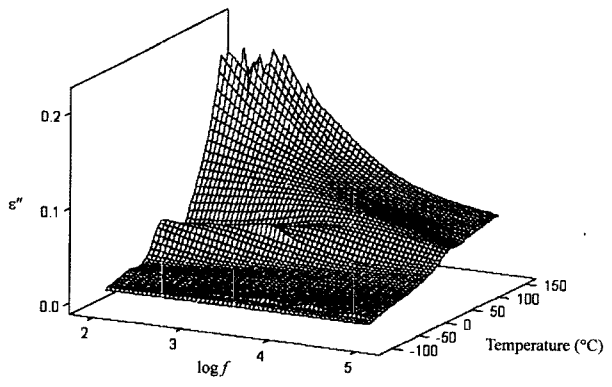

Figure 4. Dielectric loss vs frequency and temperature of the POL film.

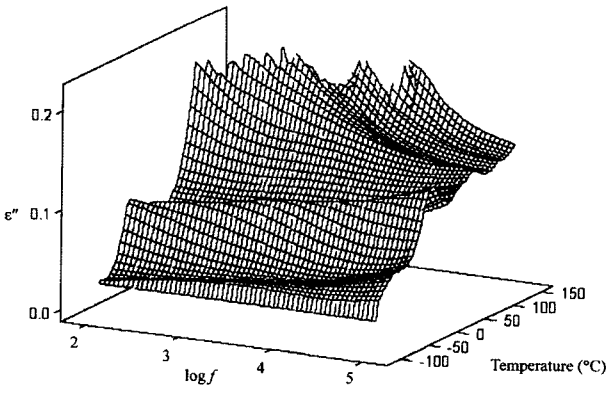

Figure 5. Dielectric loss vs frequency and temperature of the POLSA film.

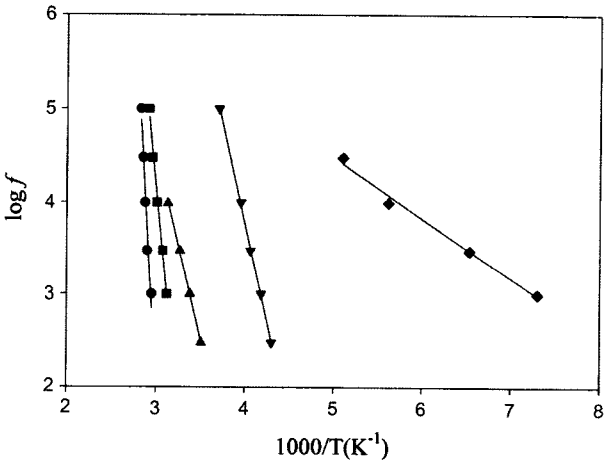

Figure 6. Temperature dependence of the relaxation frequencies for sub-T_g and T_g of the two different oriental lacquers: (●) α relaxation of POLSA, (■) α relaxation of POL, (▲) β relaxation of POL, (▼) β relaxation of POLSA, (◆) γ relaxation of POLSA.

Table II. Activation Energies of Relaxations for POL and POLSA Films

Sample	Sub-T_g		T_g	
	T (°C)	ΔE(kcal/mol)	T (°C)	ΔE(kcal/mol)
POL	1	19	50	60
	-50	-		
POLSA	-50	20	75	92
	-100	7		

relaxation at -50 °C for the POL film is too weak to be characterized. The activation energies of the relaxation peaks for the POLSA film at around 75, -50, and -100 °C were 92, 20, and 7 kcal/mol, and are labeled as α, β, and γ, respectively. The above results demonstrate how the addition of UV-curable SA into oriental lacquer affects the relaxation behavior of the oriental-lacquer coating network. In ε'' profile of POLSA film, the α relaxation peak shifted to higher temperature in comparison with the POL film and strong secondary relaxations exhibited in the range -100~-50 °C ranges due to the molecular motion of Si-O-Si. This result indicates that the UV modification of oriental lacquer by the dual curing can impart a reinforcing effect and the flexible molecular motion of Si-O-Si can provide a strong relaxation effect in the coating network. Consequently, it can be assumed that the coating produced by the POLSA film is tougher and harder than that with the POL film. Our pendulum and pencil hardness data support this explanation.

Valuable information on the dielectric relaxation process can be obtained from examination of the shape of the Cole-Cole plots of ε'' and ε'. The frequency- and temperature-dependent complex dielectric constant is given by

$$\varepsilon^*(\omega, T) = \varepsilon'(\omega, T) - i\varepsilon''(\omega, T) \quad (1)$$

where ω is the angular frequency, T is the temperature, and $i=(-1)^{1/2}$.

It is common practice to characterize dielectric parameters by the real part of the dielectric constant and by the imaginary part of the dielectric loss factor. In general, the dielectric constant as a function of the frequency at a given temperature can be described mathematically by the empirical Havriliak-Negami equation, which is applicable to the dielectric relaxation process for most polymers.[11]:

$$\varepsilon^* = \varepsilon_\infty + \frac{\varepsilon_o - \varepsilon_\infty}{\{1+(i\omega\tau)^\alpha\}^\beta} \quad (2)$$

where ε^* is the complex dielectric constant, ε_o and ε_∞ represent the relaxed ($\omega \rightarrow 0$) and unrelaxed ($\omega \rightarrow \infty$) values of the dielectric constant, ω is the frequency, τ is the relaxation time, and α and β represent the distribution and skewing parameters, respectively. When $\alpha = 1$, eq. (1) reduces to the Davidson-Cole expression corresponding to a dispersion in the shape of a skewed semicircle, while for $\beta = 1$ a symmetric arc results (the Cole–Cole form). When both α and β are equal to unity, the Debye expression is recovered.[12,13]

The Cole-Cole plots were constructed at selected temperatures in the vicinity of relaxation regions, and are shown in Figures 7 and 8 for the POL and POLSA films, respectively. For both films, the Cole-Cole plots are well fitted by the Havriliak–Negami equation. The shapes of the Cole-Cole plots at 1 °C for the POL film and at -50 °C for the POLSA film are asymmetrical, being broader in the high-frequency region, suggesting that another relaxation mode exists. In

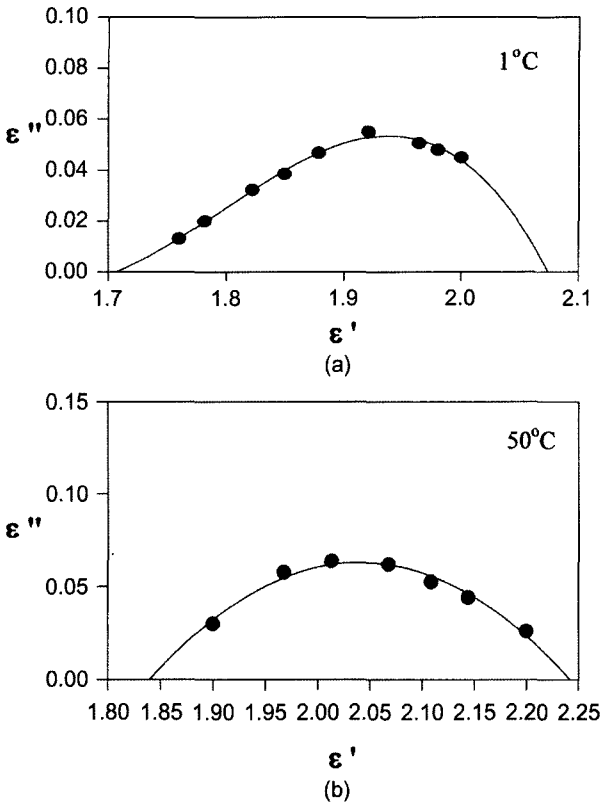

Figure 7. Cole-Cole plots of the POL film at different temperatures.

the α relaxation region for the POL and POLSA films, the shape of the Cole-Cole plot at 80 °C for the POLSA film is also asymmetrical, although it is more symmetric than that of the relaxation at the low-temperature region. For the relaxation at 50 °C of the POL film, however, a more-symmetric response is observed. These results suggest that the relaxation behavior of the POLSA film is very different from that of the POL film due to microstructural differences between the two coating networks. It could be expected that the POLSA film has more than two relaxations in the α relaxation region due to the existence of various cross-linked windows resulting from the dual curing mechanisms; namely UV-curable SA and conventional oriental-lacquer curing, even though the POLSA film shows a single glass transition. This result reflects that the POLSA film can have the nano or micro inhomogeneous coating networks.[14]

The parameters included in eq. (2) were determined at each temperature of interest by a least-squares curve-fitting approach, using the initial values for the parameters[15,16] as summarized in Table III. The distribution and skewing parameters of the POL and POLSA films increase with increasing temperature, with the exception of the low-temperature region of the POLSA film. This result reflects a gradually narrowing distribution of the relaxation time, which demonstrates that the molecular mobility of each molecular segment

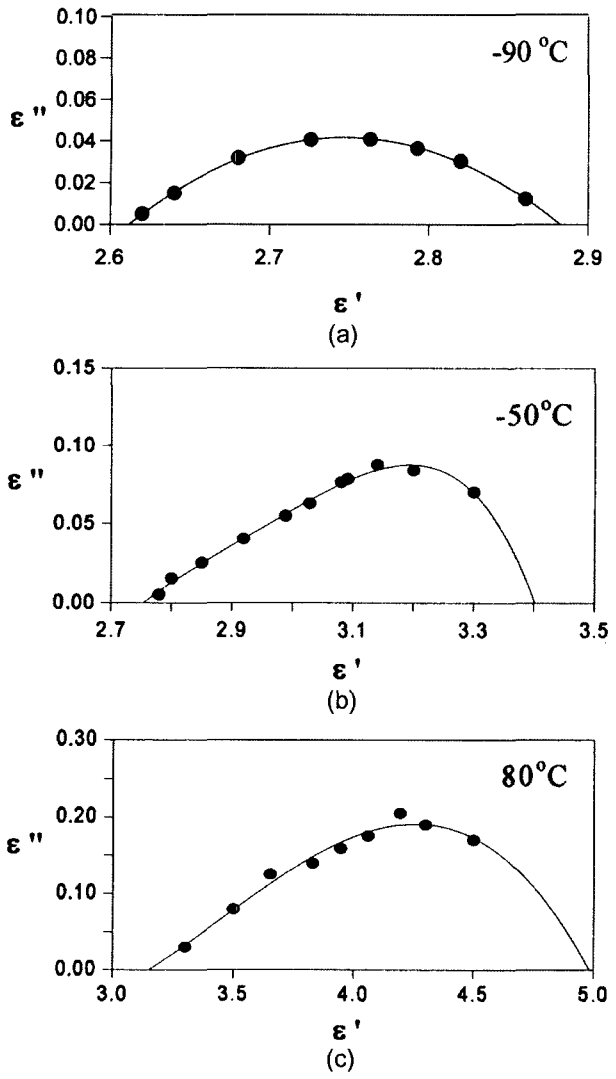

Figure 8. Cole-Cole plots of the POLSA film at different temperatures.

reaches the same level and approaches a single relaxation time.[17] In the low-temperature region of the POLSA film, however, the increase in the distribution parameter is probably due to local relaxation motion of side chains or groups, which may exhibit thermal motion that is almost independent of that of the main chain. It may also be attributable to the activation energy of sub-T_g for the POLSA film at around -100 °C. It is interesting to note that the skewing parameter value of the POLSA film is lower than that of the POL film in the α relaxation region, suggesting that different relaxation modes exist in the coating networks of the POL and POLSA films.

The dielectric intensities were obtained by determining the intersection point of the circle with the ε' axis in each of the Cole-Cole plots at the different temperatures.[18] The dielectric relaxation intensity $\Delta\varepsilon$ is defined as

$$\Delta\varepsilon(T) = \varepsilon_0(T) - \varepsilon_\infty(T) \quad (3)$$

Table III. Values of the Parameters Given by the Model (Havriliak-Negami Equation) for POL and POLSA Films

Sample	Temperature (°C)	$\Delta\varepsilon$	α	β	Relaxation Time (s)
POL	-50	0.13	0.29	0.18	5.5×10^{-2}
	-48	0.17	0.32	0.19	4.9×10^{-2}
	-46	0.19	0.35	0.21	4.3×10^{-2}
	-1	0.32	0.38	0.27	7.2×10^{-3}
	1	0.37	0.40	0.29	4.4×10^{-3}
	50	0.43	0.41	0.31	1.2×10^{-3}
	52	0.64	0.51	0.61	8.8×10^{-4}
	54	0.71	0.53	0.62	7.5×10^{-4}
POLSA	-90	0.27	0.64	0.54	3.8×10^{-3}
	-97	0.29	0.67	0.55	3.4×10^{-3}
	-95	0.30	0.68	0.57	3.2×10^{-3}
	-50	0.65	0.29	0.25	6.8×10^{-3}
	-48	0.67	0.31	0.26	3.9×10^{-3}
	-46	0.69	0.34	0.27	2.3×10^{-3}
	78	1.79	0.61	0.34	1.3×10^{-3}
	80	1.82	0.65	0.36	7.8×10^{-4}
	82	1.84	0.67	0.38	3.2×10^{-4}

where $\Delta\varepsilon$ is the difference between ε_o, the relaxed dielectric constant for the low-frequency region, and ε_∞, the unrelaxed dielectric constant for the high-frequency region. This characterizes the mobility and number of molecular dipoles. The relaxation intensities $\Delta\varepsilon$ for the POL and POLSA films increase with increasing temperature. An increase in the molecular mobility causes the dipoles to reorient toward the alternating electric field, thereby resulting in an increase of the relaxation intensities.[19,20] In addition, consideration of the dielectric intensity values of both samples reveals a stronger dipolar response for the POLSA film than for the POL film. The weaker relaxation of the POL film indicates that it involves fewer dipoles than that in the POLSA film. It is also expected that the densely packed grain structure of the POL film could be affected by the neighboring molecules, which restricts the relaxation process. However, the fact that there are many Si-O-Si groups whose mobility and rotation are relatively easy in the coating network of the POLSA film provides a reasonable explanation for the increased dielectric relaxation intensity.[21-23]

Conclusions

It has been demonstrated that the introduction of 5 wt% UV-curable SA into the oriental lacquer formulation and the dual curing (UV and typical oriental lacquer) process led to the formation of films that were quite different from conventional oriental lacquer films.

The combination of UV curing and conventional oriental-

lacquer curing made it possible to produce a 77 μm-thick film using a one-step drying procedure. We believe that the presence of silicone groups in the oriental-lacquer coating network made oxygen diffusion possible, which subsequently led to the oxidation-induced cross-linking of the oriental lacquer in both the core and film-substrate regions.

Dielectric data show that the POL film cured by the traditional process exhibits sub-T_g relaxation at -50 and 1 °C, and α relaxation at 50 °C. However, the POLSA film, modified by UV-curable SA, exhibits sub-T_g relaxations at around -100 and -50 °C, and α relaxation at 75 °C. This suggests that the POLSA film could provide a coating that is tougher and harder than for POL film. The experimental data fit the Havriliak-Negami equation well. For both POL and POLSA, this analysis gave the temperature-dependent values of the relaxation time and relaxation strength $\Delta\varepsilon$. The value of $\Delta\varepsilon$ for the POL film is lower than that for the POLSA film, revealing that the relaxation of the POL film involves fewer dipoles than that of the POLSA film. Due to the densely packed grain structure of the POL film, its relaxation process can be restricted by the neighboring molecules. However, the presence of many Si-O-Si groups whose mobility and rotation are relatively easy in the coating network of POLSA provides a reasonable explanation for the increased dielectric relaxation intensity in that coating network. In addition, the POLSA film has the local relaxation motion of side chains or groups, which may exhibit thermal motion that is almost independent of that of the main chain at around -100 °C. Consequently, it is suggested that the excellent toughness of the POLSA film originates from the special microstructure of the coating network, where various secondary relaxations including relaxation of siloxane group modes permit sufficient subgroup motion to allow deformation. FTIR-ATR and film hardness data support this conclusion.

Acknowledgements. This study was supported by research funds from Chosun University in 2006.

References

(1) D. M. Snyder, *J. Chem. Edu.*, **66**, 977 (1989).
(2) T. Nakamura, *Biochem. Biophysics Res. Commun.*, **2**, 111 (1960).
(3) M. Takada, R. Oshima, Y. Yamauchi, J. Kumanotani, and M. Seno, *J. Org. Chem.*, **53**, 3072 (1988).
(4) W. H. Daly and S. Moulay, *J. Polym. Sci. Polym. Symp.*, **74**, 227 (1986).
(5) J. Kumanotani, *J. Macromol. Chem.*, **179**, 47 (1978).
(6) E. Obataya , Y. Furuta, Y. Ohno, M. Norimoto, and B. Tomita, *J. Appl. Polym. Sci.*, **83**, 2288 (2002).
(7) R. Oshima, Y. Yamauchi , C. Watanabe, and J. Kumanotani, *J. Org. Chem.*, **50**, 613 (1985).
(8) H. W. Starkweather, *Macromolecules*, **14**, 1277 (1981).
(9) A. Livi, G.. Levita, and P. A. Rolla, *J. Appl. Polm. Sci.*, **50**, 1583 (1993).
(10) G. Hoffmann and S. Poliszko, *J. Appl. Polym. Sci.*, **59**, 269 (1996).
(11) B. A. Bedeker, Y. Tsujii, N. Ide, Y. Kita, T. Fukuda, and T. Miyamoto, *Polymer*, **36**, 4735 (1995).
(12) M. Younes, S. Wartewig, D. Lellinger, B. Strehmel, and V. Strehmel, *Polymer*, **35**, 5269 (1994).
(13) J. W. Hong, H. K. Kim, and J. O. Choi, *J. Appl. Polym. Sci.*, **76**, 1804 (2000).
(14) G. Katana, E. W. Fischer, Th. Hack, V. Abetz, and F. Kremer, *Macromolecules*, **28**, 2714 (1995).
(15) R. H. M. Leur, *Polymer*, **35**, 2691 (1994).
(16) I. Alig and G.. P. Johari, *J. Polym. Sci. Polym. Phys. B*, **31**, 299 (1993).
(17) M. S. Graff and R. H. Boyd, *Polymer*, **35**, 1797 (1994).
(18) G. H. Hsiue, R. H. Lee, R. J. Jeng, and C. S. Chang, *J. Polym. Sci. Part B*, **34**, 555 (1996).
(19) J. F. Bristow and D. S. Kalika, *Macromolecules*, **27**, 1808 (1994).
(20) R. D. Calleja, I. Devine, L. Gargallo, and D. Radić, *Polymer*, **35**, 151 (1994).
(21) J. S. Hwang, J. Lee, and Y. H. Chang, *Macromol. Res.*, **13**, 409 (2005).
(22) S. Y. Pyun and W. G. Kim, *Macromol. Res.*, **11**, 202 (2003).
(23) T. Das, A. K. Banthia, and B. Adhikari, *Macromol. Res.*, **14**, 261 (2006).